Developmental Cell, Volume *25*

Supplemental Information

The Hippo Effector Yorkie Controls

Normal Tissue Growth by Antagonizing

Scalloped-Mediated Default Repression

Laura M. Koontz, Yi Liu-Chittenden, Feng Yin, Yonggang Zheng, Jianzhong Yu, Bo Huang, Qian Chen, Shian Wu, and Duojia Pan

Inventory of Supplemental Information

Supplemental Figures

Figure S1. Identification of Tgi by two complementary screens, related to Figure 2.

(A) Schematic of the *tgi* locus, showing the intron/exon structure of the gene. Also shown are the insertion sites of P[GS]^{cg10741} recovered from our overexpression screen and P[EPgy2]^{EY11948}, a P-element line used for imprecise excision to generate the $tgi^{\Delta P}$ allele, as well as the DNA deleted in the $tgi^{\Delta P}$ allele. RA and RB transcripts are produced by alternative splicing: they differ in the first coding exon (exon 2 vs. exon 3) but share the bulk of the protein (exons 4 and 5) including the PPxY motifs and Tondu domains. $tgi^{\Delta P}$ is predicted to delete exons 4 and 5.

(B) Schematic protein structure of *Drosophila* Tgi and its human orthologue Vgl-4. The Tondu domains (T1, T2) and PPxY motifs (P1, P2, P3) are highlighted.

(C) Overexpression of p[GS]^{cg10741} or UAS-Tgi (RB) by GMR-Gal4 resulted in eye undergrowth.

(D) Overexpression p[GS]^{cg10741} or UAS-Tgi by Vg-Gal4 (RA or RB) resulted in wing undergrowth. The graphs show quantification of wing size and wing cell density (mean ± SEM, n>=8 for each genotype). *** denotes a p-value < 1.0E-5. There is no statistical difference in wing cell density among all the genotypes (p>0.1).

(E) Summary of cell-based RNAi screen. Left: constructs used in the screen. Right: a scatter plot showing the averaged *Z* scores of all genes, with each gene represented by a single dot. The location of *cg10741*, *sd* and *yki* are marked. See Table S1 for a list of top hits from the RNAi screen.

Figure S1

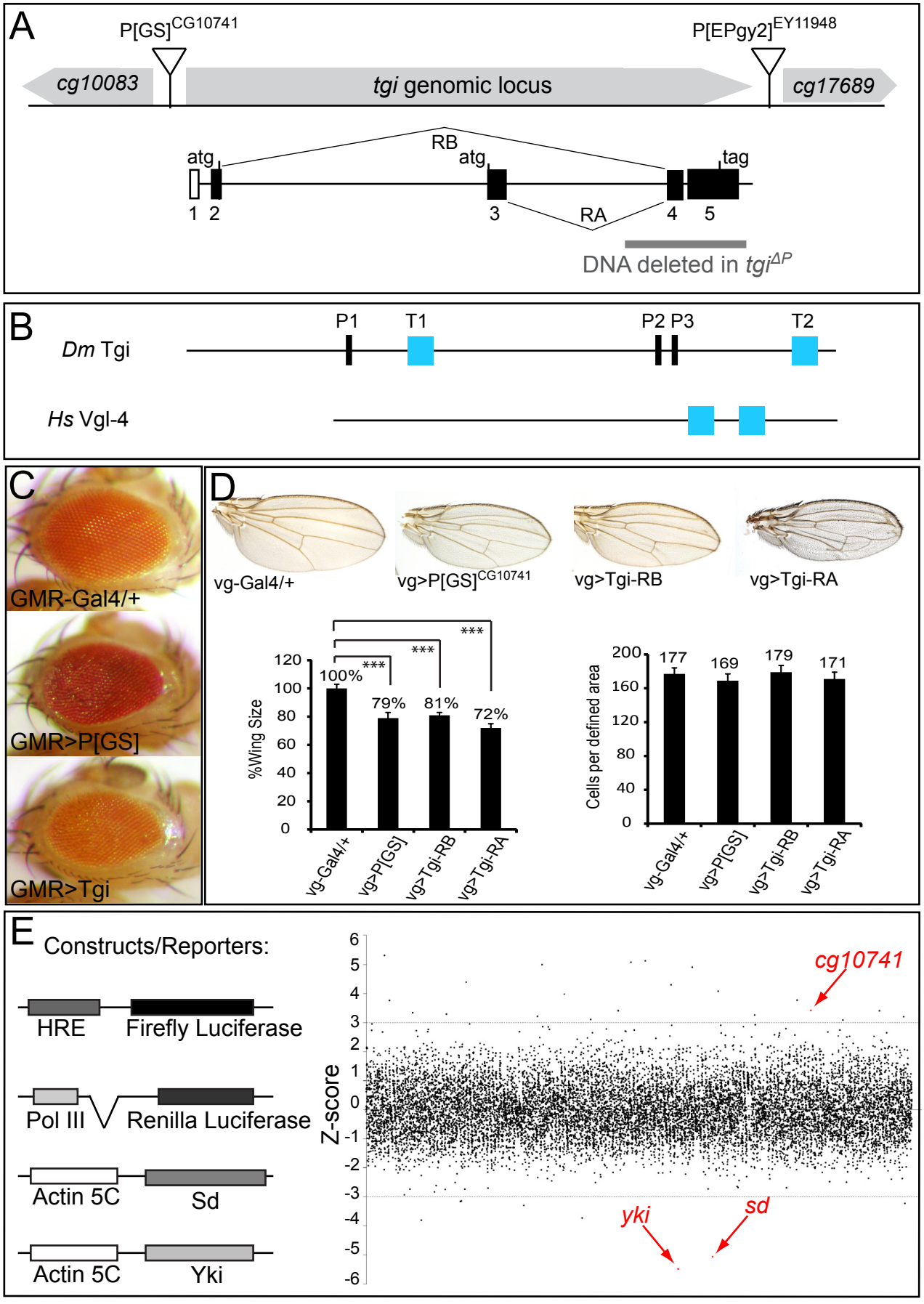
A
P[GS]CG10741
P[EPgy2]EY11948
cg10083
tgi genomic locus
cg17689
atg
RB
atg
tag
1 2
3
RA
4 5
DNA deleted in tgiΔP
B
Dm Tgi
P1
T1
P2 P3
T2
Hs Vgl-4
C
GMR-Gal4/+
GMR>P[GS]
GMR>Tgi
D
vg-Gal4/+
vg>P[GS]CG10741
vg>Tgi-RB
vg>Tgi-RA
%Wing Size
100%
79%
81%
72%
***
Cells per defined area
177
169
179
171
E
Constructs/Reporters:
HRE
Firefly Luciferase
Pol III
Renilla Luciferase
Actin 5C
Sd
Actin 5C
Yki
Z-score
cg10741
yki
sd

Figure S2. Specificity of Tgi on target gene expression and genetic interactions between Tgi and Yki/Sd, related to Figure 2.

(A) RT-PCR analysis of Tgi mRNA levels from the indicated tissue source, showing that Tgi is widely expressed. A primer pair spanning the last two exons was used to amplify an 1139 bp product. Rp49 was used as internal control for RT-PCR.

(B) RNA in situ hybridization with anti-sense (as) probe showing ubiquitous expression of *tgi* in eye and wing discs. Sense (s) probe serves as negative control.

(C-D) Tgi overexpression does not affect the expression of Vg targets. Wing discs from *dpp*-Gal4 UAS-GFP; UAS-Tgi flies were stained for Vg (C) and Dll (D). GFP signal demarcates the stripe of cells that express *dpp*-Gal4 (arrowheads).

(E-F) Vg overexpression does not phenocopy Tgi overexpression. Wing disc (E) or eye disc (F) containing Flp-out clones overexpressing Vg (GFP-positive) and stained for Diap1. Unlike Flp-out clones with Tgi overexpression, Vg overexpression clones never showed reduction in Diap1 expression. Some clones even showed increased Diap1 signal (arrowheads).

(G) Adult heads from the indicated genotypes, showing that Tgi overexpression greatly suppressed eye overgrowth resulting from Yki or Sd+Yki overexpression, and completely reverted lethality associated with Sd+Yki overexpression (from 19 to 100% viability).

(H) Adult eyes from the indicated genotypes, showing that *yki* heterozygosity further decreased the eye size in GMR-Gal4; UAS-Tgi background.

(I) Adult wings from the indicated genotype showing genetic interactions between Tgi and Yki-Sd. The graph shows quantification of wing size relative to Vg-Gal4/+ control (mean ± SEM, n>=8 for each genotype). Yki heterozygosity further decreases wing size in the Vg-Gal4; UAS-Tgi background (81 ± 1% vs. 71 ± 1%; p=3.7E-5). There is no significant difference in the wing undergrowth caused by Tgi or Sd overexpression (81 ± 1% vs. 79 ± 1%; p=0.45). Co-overexpression of Sd further decreases eye size in the GMR-Gal4; UAS-Tgi background (81 ± 1% vs. 32 ± 1%; p=2.3E-9).

Figure S2

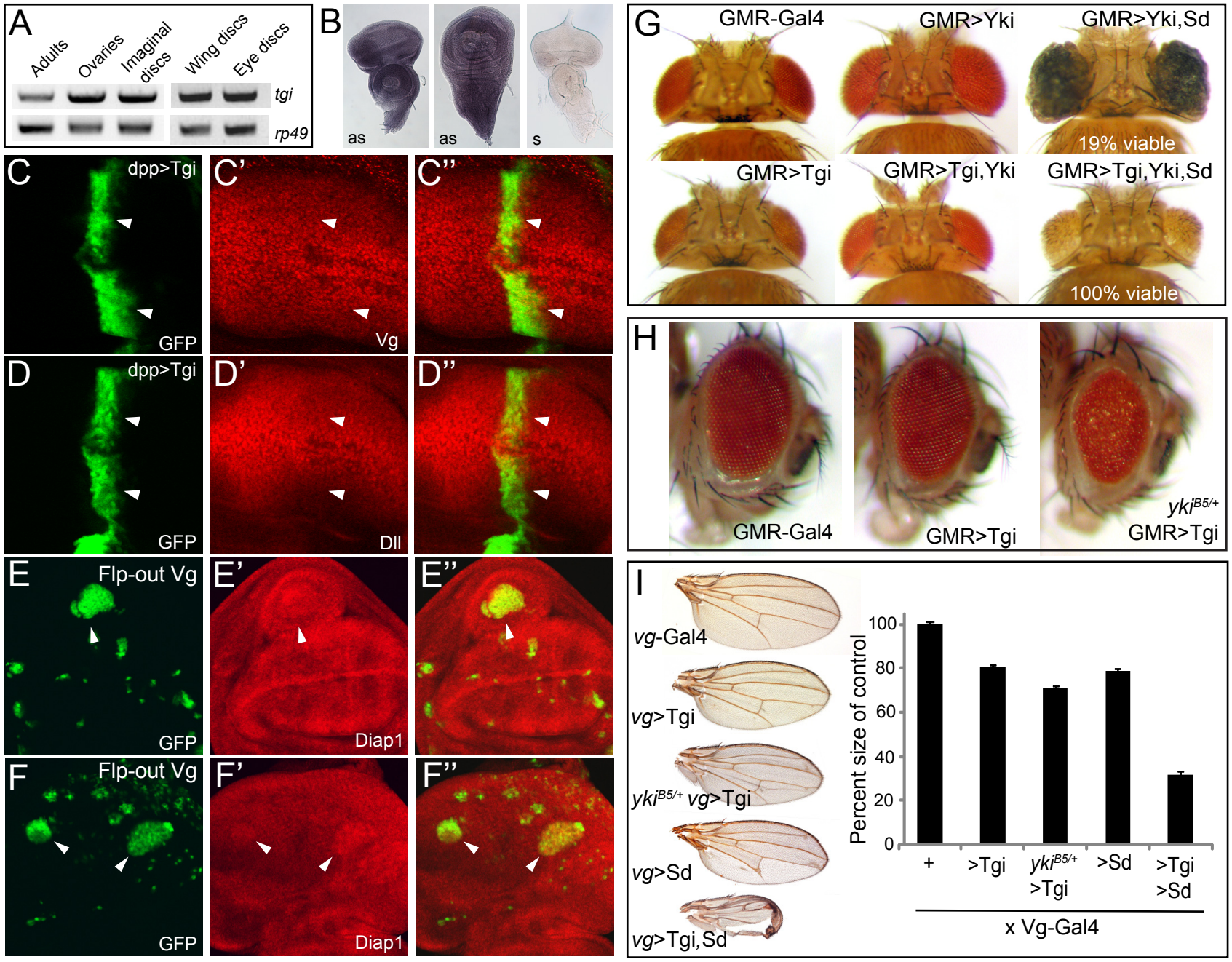
A
Adults
Ovaries
Imaginal discs
Wing discs
Eye discs
tgi
rp49
B
as
as
s
C
dpp>Tgi
GFP
C'
Vg
C''
D
dpp>Tgi
GFP
D'
Dll
D''
E
Flp-out Vg
GFP
E'
Diap1
E''
F
Flp-out Vg
GFP
F'
Diap1
F''
G
GMR-Gal4
GMR>Yki
GMR>Yki,Sd
19% viable
GMR>Tgi
GMR>Tgi,Yki
GMR>Tgi,Yki,Sd
100% viable
H
GMR-Gal4
GMR>Tgi
ykiB5/+
GMR>Tgi
I
vg-Gal4
vg>Tgi
ykiB5/+ vg>Tgi
vg>Sd
vg>Tgi,Sd
Percent size of control
100
80
60
40
20
0
+
>Tgi
ykiB5/+ >Tgi
>Sd
>Tgi >Sd
x Vg-Gal4

Figure S3. Mutation of the Tondu domains, but not of the PPxY motifs, abolishes Tgi-induced Diap1 downregulation, related to Figure 3.

(A-D) Wing discs from *dpp*-Gal4 UAS-GFP (A), UAS-HA-Tgi; *dpp*-Gal4 UAS-GFP (B), UAS-HA-Tgi^{T12}; *dpp*-Gal4 UAS-GFP (C), or UAS-HA-Tgi^{P123}; *dpp*-Gal4 UAS-GFP flies, showing GFP and Diap1 expresssion. Arrowheads mark the *dpp*-expressing stripe in the wing discs. Note the reduced Diap1 expression in the *dpp* stripe resulting from Tgi overexpression (compare A and B). Overexpression of Tgi^{T12} had no effect on Diap1 expression in the *dpp* strip (C), but overexpression of Tgi^{P123} clearly decreased Diap1 expression in the *dpp* stripe (D). All transgenes were inserted at an identical chromosomal location.

(E) Tgi is a nuclear protein. High magnification view of wing disc from *dpp*-Gal4 UAS-GFP; UAS-HA-Tgi flies stained with DNA dye DAPI and antibody against HA. Note the co-localization of the HA-Tgi signal with the nuclear DAPI signal.

(F) Tgi inhibited Yki-driven HRE luciferase activity as well as binding of Yki to the HRE. (left) luciferease assay in S2R+ cells expressing the indicated expression constructs. Error bars represent standard deviations. Note the suppression of Sd/Yki-activated HRE activity by Tgi. (right) ChIP assay in S2R+ cells examining Yki binding to the endogenous HRE. Chromatins were precipitated from lysates of S2R+ cells expressing the indicated combination of plasmids using anti-HA antibody. A ~100bp DNA (+3993-+4101) encompassing the HRE was amplified following ChIP. The region -3536 to -3430 (marked as 5'con) that doesn't contain any putative Sd-binding site was used as a negative control region for PCR. The HRE amplicon was recovered only in the presence of Yki+Sd, and the expression of Tgi reduced the amount of HRE amplicon.

Figure S3

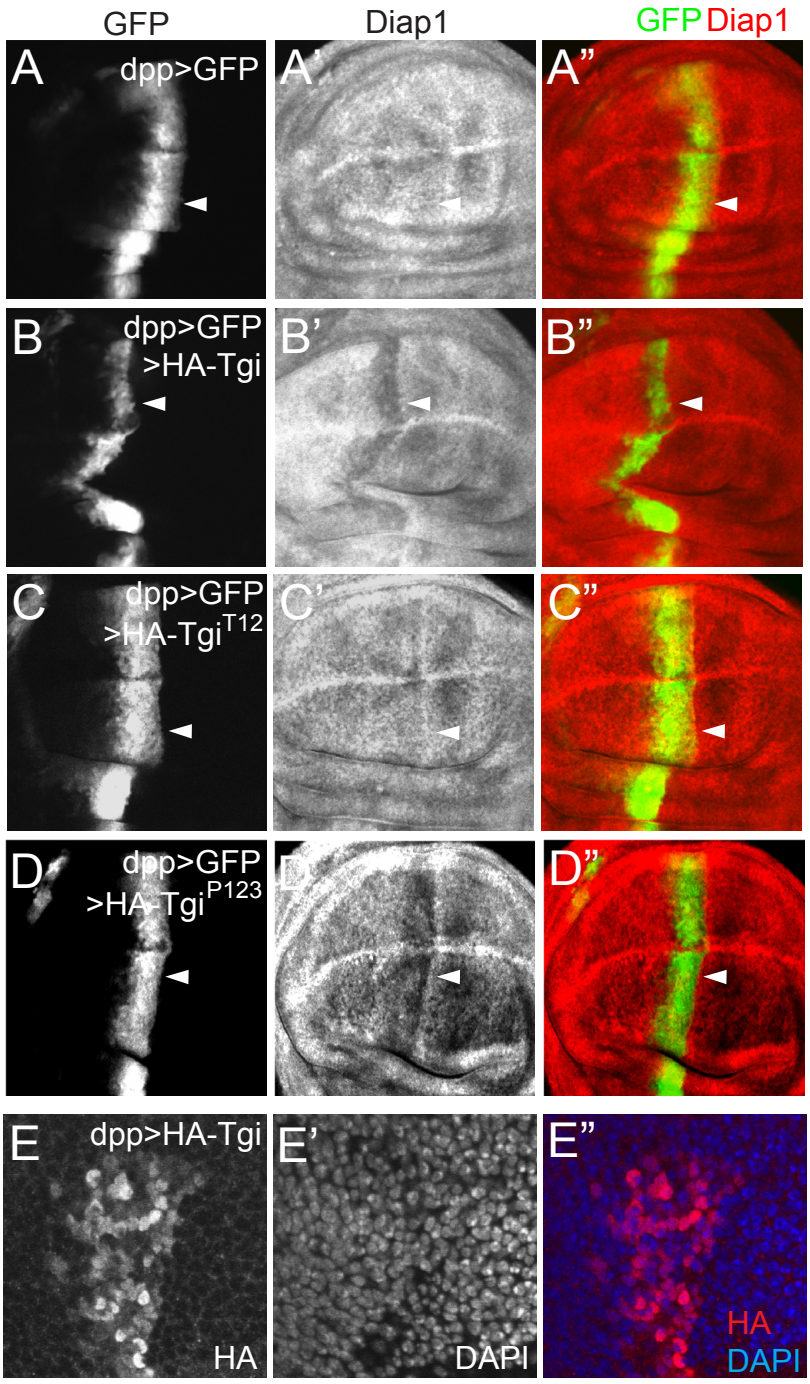
GFP
Diap1
GFP Diap1
A
dpp>GFP
A'
A"
B
dpp>GFP
>HA-Tgi
B'
B"
C
dpp>GFP
>HA-Tgi^T12
C'
C"
D
dpp>GFP
>HA-Tgi^P123
D'
D"
E
dpp>HA-Tgi
HA
E'
DAPI
E"
HA
DAPI

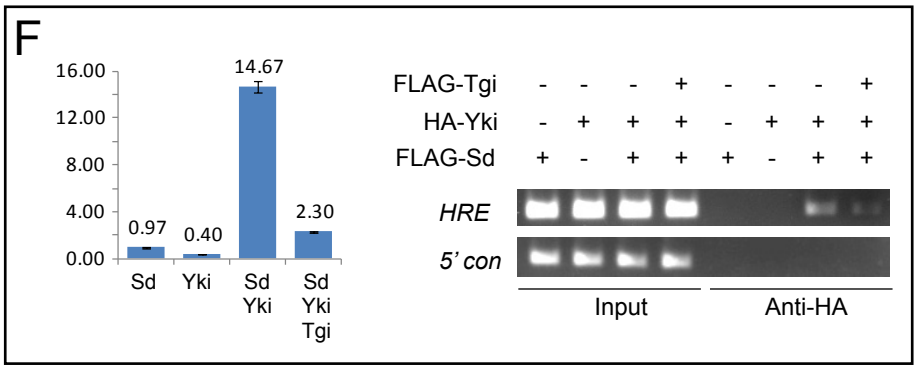
F
16.00
12.00
8.00
4.00
0.00
0.97
0.40
14.67
2.30
Sd
Yki
Sd Yki
Sd Yki Tgi
FLAG-Tgi - - - + - - - +
HA-Yki - + + + - + + +
FLAG-Sd + - + + + - + +
HRE
5' con
Input
Anti-HA

Figure S4. Loss of Tgi does not affect clonal growth or Hippo target gene expression, related to Figure 4.

In all panels, *tgi*$^{\Delta P}$ mutant clones were marked as GFP- or β-Gal-negative as indicated.

(A-K) Wing discs (A, C, E, G, H, J) and eye discs (B, D, F, I, K) containing *tgi*$^{\Delta P}$ mutant clones were stained for *diap1-lacZ* (A-B), *ex-lacZ* (C-D), *fj-lacZ* (E-F), Vg (G), Yki (H-I), Sd-GFP (J-K). Note the normal expression of *diap1*, *ex*, *fj*, Vg, Yki and Sd-GFP in *tgi*$^{\Delta P}$ clones (arrowheads). Also note the comparable size of *tgi*$^{\Delta P}$ mutant clones (marker-negative) compared to adjacent twin spots (2xmarker).

(L) Endogenous Sd expression as reported by the Sd-GFP protein trap line CA07575 (Neto-Silva et al., 2010). In this line, GFP is spliced in-frame with Sd to produce functional Sd-GFP fusion proteins. Sd-GFP is expressed throughout the eye and the wing disc, with the wing pouch showing elevated levels of expression. The Sd-GFP protein trap line more faithfully reports the endogenous Sd expression pattern than the commonly referred lacZ enhancer trap line inserted upstream of the coding exons (Sd^{ETX4}) (Campbell et al., 1992).

Figure S4

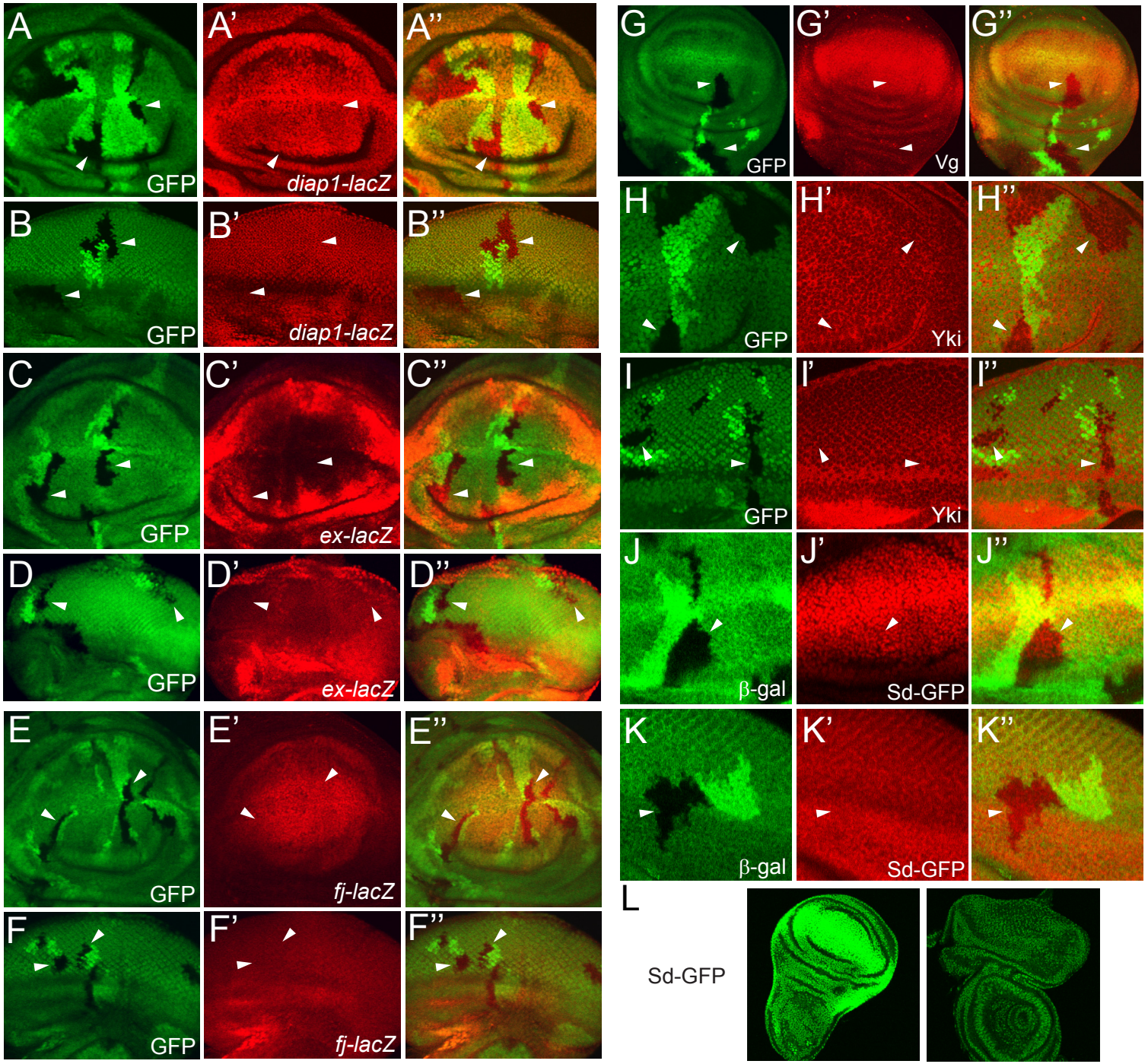
A
GFP
A'
diap1-lacZ
A''
B
GFP
B'
diap1-lacZ
B''
C
GFP
C'
ex-lacZ
C''
D
GFP
D'
ex-lacZ
D''
E
GFP
E'
fj-lacZ
E''
F
GFP
F'
fj-lacZ
F''
G
GFP
G'
Vg
G''
H
GFP
H'
Yki
H''
I
GFP
I'
Yki
I''
J
β-gal
J'
Sd-GFP
J''
K
β-gal
K'
Sd-GFP
K''
L
Sd-GFP

Figure S5. Loss of *sd* or *tgi* affects Grk localization in the oocyte, related to Figure 5.

(A) Temporal regulation of Hippo signaling in oogenesis. Composite image of *Drosophila* egg chambers from stage 1 (S1) to stage 9 (S9), showing the maturation of egg chambers and temporal regulation of Hippo signaling. The egg chambers were stained with Cut (red) and the DNA dye DAPI (blue). In stages 1-6, follicle cells undergo mitotic proliferation, Hippo signaling is off, Yki is active, and Cut is expressed. Between stage 7 and stage 9, follicle cells undergo endoreplicative growth, Hippo signaling is on, Yki is inactive, and Cut expression is off.

(B-F) stage 7-9 wildtype (B) and mutant egg chambers containing PFC mutant clones of *hpo* (C), *mer* (D), *sd* (E) and *tgi* (F). Mutant clones were marked as GFP-negative. Note the mislocalization of Grk from the dorsal anterior corner to the posterior pole of the mutant oocyte (compare arrowheads). Also note the multilayering of PFCs in *hpo* and *mer*, but not *sd* or *tgi* mutant clones. Overall, the *sd* and *tgi* mutant phenotypes are weaker than those of Hippo tumor suppressors.

Figure S5

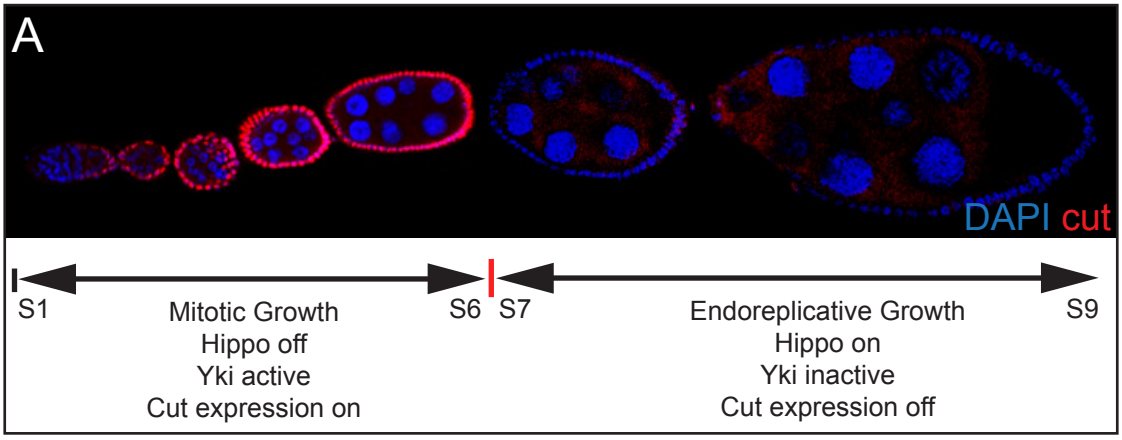
A
DAPI cut
S1
Mitotic Growth
Hippo off
Yki active
Cut expression on
S6
S7
Endoreplicative Growth
Hippo on
Yki inactive
Cut expression off
S9

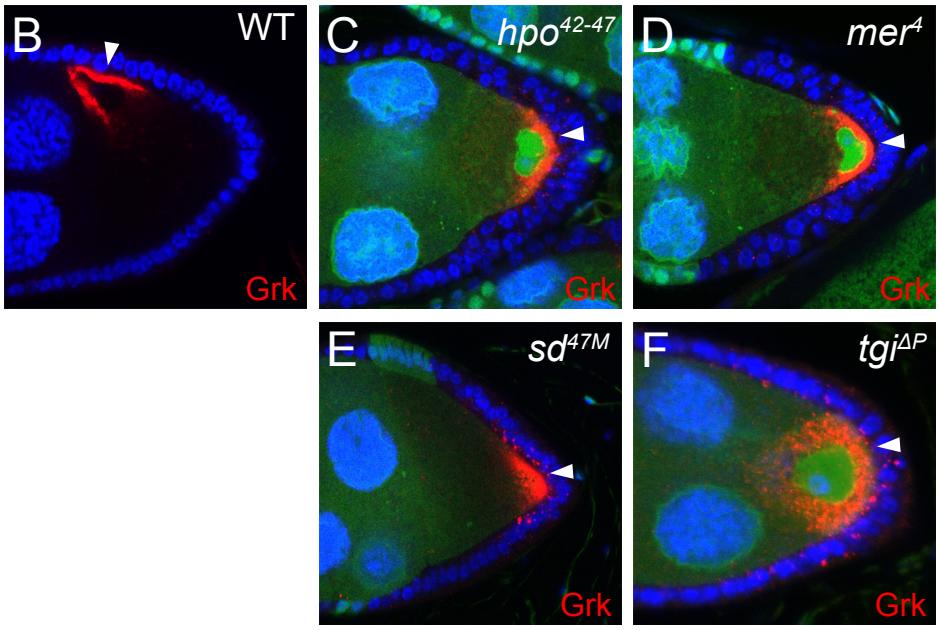
B
WT
Grk
C
hpo42-47
Grk
D
mer4
Grk
E
sd47M
Grk
F
tgiΔP
Grk

Figure S6. RNAi of Sd or Tgi does not reduce the expression of the Ex transgene, related to Figure 6.
(A-C) Eye imaginal discs of the indicated genotypes were stained for Ex protein (red). The Ex transgene is expressed at similar levels posterior to the morphogenetic furrow in the three genotypes. The specific genotypes are: (A) UAS-Dicer2; GMR-Gal4 UAS-Ex; UAS GFP RNAi (abbreviated as GMR >Ex >GFP RNAi); (B) UAS-Dicer2; GMR-Gal4 UAS-Ex; UAS Sd RNAi (abbreviated as GMR >Ex >SdRNAi); (C) UAS-Dicer2; GMR-Gal4 UAS-Ex/UAS Tgi RNAi (abbreviated as GMR >Ex >Tgi RNAi).

Figure S6

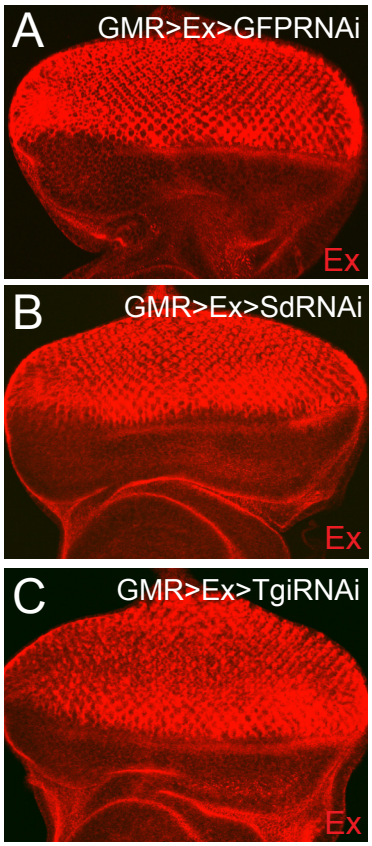

Figure S7. Vgl4 suppresses YAP-mediated transcription in cultured cells and YAP-induced transcriptional changes in transgenic livers, related to Figure 7.

(A) Phylogenetic tree of all Tondu domain-containing proteins from *Drosophila* (Vg and Tgi), Xenopus (x), mouse (m) and human (h). Note the clustering of Tgi with Vgl4 and the clustering of Vg to Vgl1, 2 and 3. Maximum likelihood tree was generated using Aligx program of VectorNTI. Gap opening penalty, gap exteinsion penalty and gap separation penalty range were set as 10, 0.05 and 8, respectively.

(B) Bi-directional co-immunoprecipitation between TEAD2 and Vgl4. HEK293 cell lyastes expressing the indicated combination of HA-TEAD2 and Myc-Vgl4 constructs were immunoprecipitated and probed with the indicated antibodies. Myc-Vgl4 was detedcted in HA-IP in the presence of HA-TEAD2. Conversely, HA-TEAD2 was detected in Myc-IP in the presence of Myc-Vgl4.

(C) Vgl4 suppressed YAP-mediated transactivation of Gal4-TEAD4. Luciferase activity was measured in triplicates in HEK293 cells transfected with the indicated constructs and plotted relative to Gal4-TEAD4. Error bars represent standard deviations.

(D) Vgl4 suppressed YAP-mediated activation of *Ctgf*-luciferase reporter. Luciferase activity was measured in triplicates in HEK293 cells transfected with the indicated constructs and plotted relative to HA-TEAD2. Error bars represent standard deviations.

(E) Vgl4, but not $Vgl4^{T12}$, physically interacts with TEAD4. HEK293 cells were transfected in duplicate with the indicated constructs and subjected to IP using anti-HA and probed by anti-Gal4.

(F) Quantitative real-time PCR analysis of gene expression in transgenic livers of the indicated genotype, following 2 weeks of 0.2 g/L Dox treatment starting at 3 weeks of age. Values are mean ±SEM, n=3. These genes represent the most highly induced genes by YAP in mouse livers that have been previously implicated in liver cancer (Dong et al., 2007). Note that Vgl4 significantly suppressed YAP-induced gene expression, with the exception of c-Myc (compare YAP Vgl4 double transgenic to YAP transgenic).

Figure S7

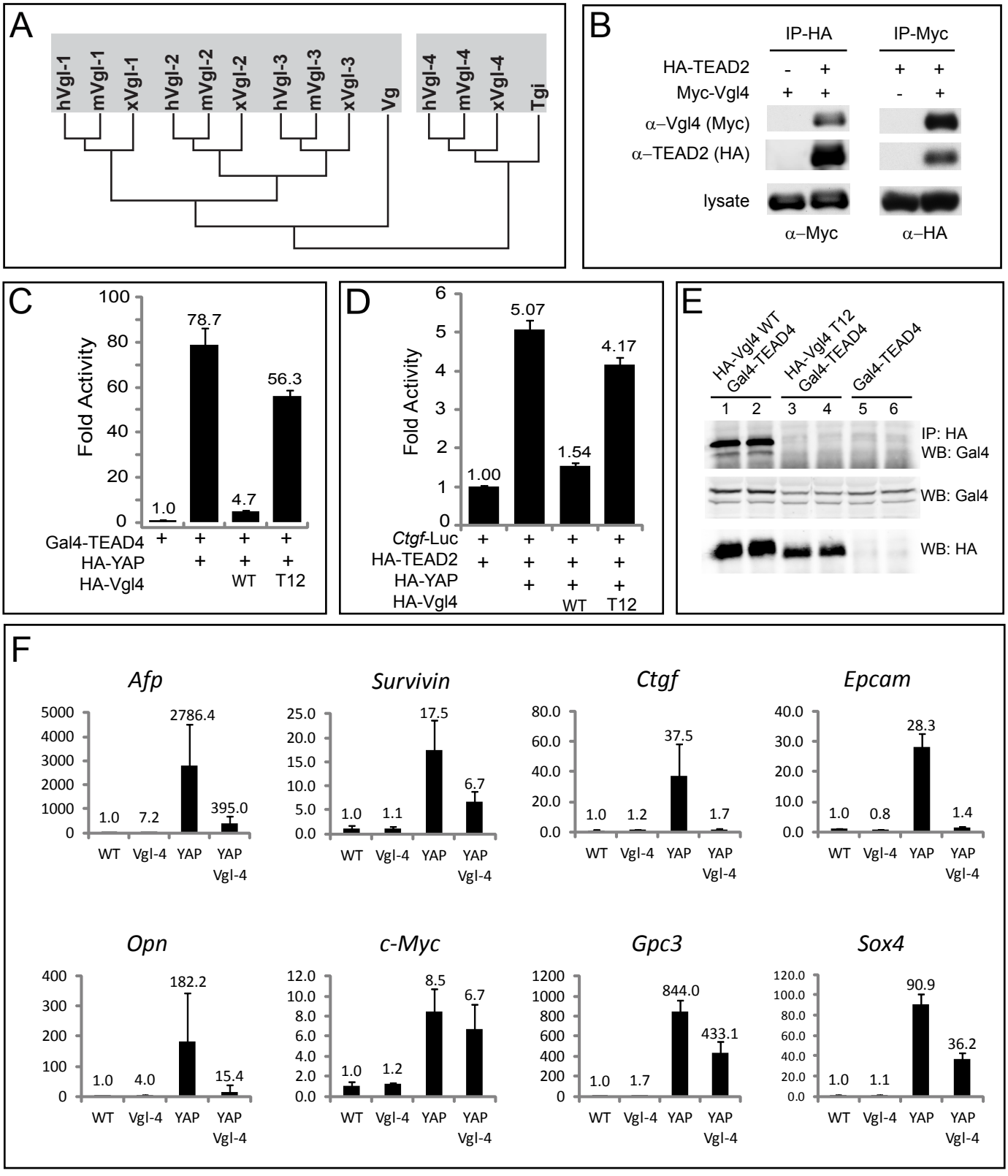
A
hVgl-1
mVgl-1
xVgl-1
hVgl-2
mVgl-2
xVgl-2
hVgl-3
mVgl-3
xVgl-3
Vg
hVgl-4
mVgl-4
xVgl-4
Tgi
B
IP-HA
IP-Myc
HA-TEAD2
Myc-Vgl4
α–Vgl4 (Myc)
α–TEAD2 (HA)
lysate
α–Myc
α–HA
C
Fold Activity
78.7
56.3
4.7
1.0
Gal4-TEAD4
HA-YAP
HA-Vgl4
WT
T12
D
Fold Activity
5.07
4.17
1.54
1.00
Ctgf-Luc
HA-TEAD2
HA-YAP
HA-Vgl4
WT
T12
E
HA-Vgl4 WT
Gal4-TEAD4
HA-Vgl4 T12
Gal4-TEAD4
Gal4-TEAD4
IP: HA
WB: Gal4
WB: Gal4
WB: HA
F
Afp
2786.4
395.0
1.0
7.2
Survivin
17.5
6.7
1.0
1.1
Ctgf
37.5
1.0
1.2
1.7
Epcam
28.3
1.0
0.8
1.4
Opn
182.2
15.4
1.0
4.0
c-Myc
8.5
6.7
1.0
1.2
Gpc3
844.0
433.1
1.0
1.7
Sox4
90.9
36.2
1.0
1.1
WT
Vgl-4
YAP
YAP Vgl-4

Supplemental Tables

Table S1. List of top hits from cell-based RNAi screen, related to Figure 2.

Hits from the genome-wide RNAi screen are ranked by Z-score and grouped into Z-score of less than -3 or greater than +3. Also shown are CG number and common gene name, if the latter is applicable. Yki, Sd, and Tgi are shown in red color. Note that the gene Pasilla is represented by two CG entries in the RNAi library, and the Z-score of both entries are shown.

Table S1

CG number	Gene name	Z-score
Z-score less than -3		
CG4005	yki	-5.48
CG8544	sd	-5.05
CG4124	PNUTS	-3.81
CG11295	l(2)dtl	-3.72
CG8580	bhr	-3.30
CG34422		-3.23
CG5848	cactus	-3.17
CG5871		-3.14
Z-score greater than 3		
CG7518		3.07
CG11879	yem-α	3.10
CG7135		3.19
CG9191	Klp61F	3.21
CG1772	decapo	3.25
CG5215	Zn72D	3.28
CG3733	dCHD1	3.33
CG4399	east	3.39
CG14644		3.41
CG10741	tgi	3.42
CG2275	jun	3.76
CG13290		3.76
CG3241	msl-2	4.08
CG8171	double parked	4.29
CG6103	CrebB-17A	4.38
CG8144 (CG16765)	pasilla	4.89 (4.17)
CG9383	asf1	4.98
CG16854		5.07
CG18009	dTRF2	5.11
CG2028	CK1α	5.29

Table S2. Schematic representation of the eukaryotic tree of life showing the distribution of Sd, Yki, Tgi and Vg homologues, related to Figure 7.

Representative species in the different taxa along evolution are illustrated. A black dot indicates the presence of a clear ortholog, while the absence of a dot indicates the lack of a clear ortholog.

Table S2

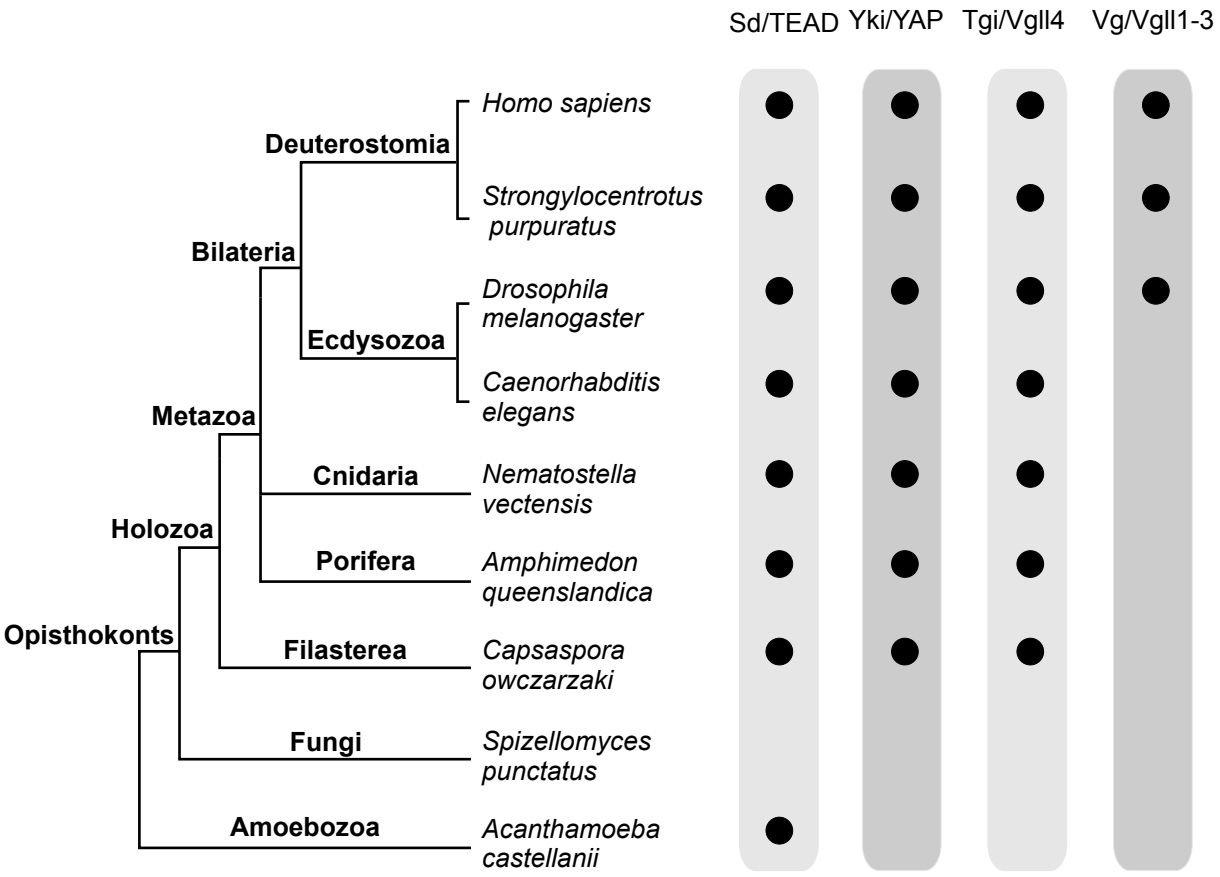
Sd/TEAD
Yki/YAP
Tgi/Vgll4
Vg/Vgll1-3
Homo sapiens
Strongylocentrotus purpuratus
Drosophila melanogaster
Caenorhabditis elegans
Nematostella vectensis
Amphimedon queenslandica
Capsaspora owczarzaki
Spizellomyces punctatus
Acanthamoeba castellanii
Deuterostomia
Bilateria
Ecdysozoa
Metazoa
Cnidaria
Holozoa
Porifera
Opisthokonts
Filasterea
Fungi
Amoebozoa

Supplemental Experimental Procedures

***Drosophila* genetics**

The following flies have been described previously: *yki*^{B5}, UAS-*yki* (Huang et al., 2005); *sd*^{47M}, UAS-*sd* and UAS-*vg* (Wu et al., 2008); UAS-*hpo* and the *diap1*-lacZ reporter, *th*^{j5c8} (Wu et al., 2003); *wts*^{X1} (Xu et al., 1995); UAS-*ex* (Hamaratoglu et al., 2006). UAS-*tgi* RNAi flies were obtained from VDRC (Dietzl et al., 2007) (transformant ID 31340). UAS-*sd* RNAi flies were obtained from Bloomington *Drosophila* Stock Center (Ni et al., 2009) (stock ID 29352). All *in vivo* RNAi experiments included UAS-Dicer2, which enhances the potency of RNAi (Dietzl et al., 2007). Full-length *tgi* cDNAs (RE45537 corresponding to the annotated RB transcript, or a PCR product corresponding to the annotated RA transcript amplified from an adult *Drosophila* cDNA library) were used to make *UAS-tgi*. *attB-UAS-HA-tgi* transgenes were made by cloning wild type, Tondu domain mutants and PPxY mutants into the attB-UAS vector. *attB-UAS-vgl4* wildtype and Tondu domain mutant flies were also constructed. All *attB-UAS* constructs were recombined into the 51C *attP* acceptor site (Bischof et al., 2007).

For MARCM and Flp-out experiments, all clones were induced 68-72 hours after egg deposition and heat-shocked at 38°C for 30 minutes unless otherwise indicated.

hs-FLP; Act>c2>Gal4 UAS-GFP;UAS-tgi th^{j5c8}

hs-FLP; Act>c2>Gal4 UAS-GFP/ex^{e1}*;UAS-tgi*

hs-FLP; Act>c2>Gal4 UAS-GFP/UAS-vg (10 minutes)

UAS-GFP hs -FLP; tub-Gal4; tub-Gal80 FRT82B/FRT82B

UAS-GFP hs-FLP; tub-Gal4; tub-Gal80 FRT82B/FRT82B wts^{X1} (5 minutes)

UAS-GFP hs-FLP; tub-Gal4/UAS-tgi; tub-Gal80 FRT82B/FRT82B wts^{X1}

UAS-GFP hs-FLP; tub-Gal4/UAS-tgi; tub-Gal80 FRT82B/FRT82B

tub-Gal80 FRT19A/FRT19A sd^{47M}*; UAS-GFP hs-FLP*

tub-Gal80 FRT19A/FRT19A sd^{47M}*; UAS-GFP hs-FLP/ UAS-tgi*

For conventional heatshock-induced FLP-FRT mutant clones in eye and wing discs, animals were heatshocked for one hour 48-72 hours after egg deposition for one hour. Double mutant clones in the eye imaginal discs were generated using double GFP-FRT /RFP-FRT stocks containing *ey-FLP*. Double or single mutant clones in follicle cells were generated using *hs-FLP* and double GFP-FRT or single GFP-FRT chromosomes by heat-shocking either third instar larvae or adult flies for one hour two days in a row and then feeding the adult females wet yeast paste for several days prior to ovary dissection.

Mouse genetics

To create the Tet-ON inducible Vgl4 transgenic mouse, the full-length Vgl4 cDNA was cloned into the pTRE2 vector (BD Biosciences). The TRE-Vgl4 transgene was excised from the vector and injected into fertilized (C57Bl/6 × SJL) F2 hybrid mouse eggs. Four founders were identified and crossed with an ApoE-rtTA transgenic line, and the founder with the strongest Vgl4 expression was selected. Dox-induced transgene induction was carried out as described (Dong et al., 2007). For all experimental conditions, at least three mice were used to calculate average liver/body ratio and standard deviation.

To overexpress Vgl4 in *Nf2* mutant background, *Alb-cre*/+; $NF2^{flox2/flox2}$; *ROSA26-loxP-STOP-loxP-rtTA*/+ mice were crossed with $NF2^{flox2}$/+; *ROSA26-loxP-STOP-loxP-rtTA*/+; *TRE-Vgl4*/+ mice. The pregnant females were fed with 1g/L Dox in drinking water supplemented with 2.5% sucrose starting from E11.5, and the progenies were sacrificed at birth (P0) to access liver phenotype. Livers sections from littermates of the various genotypes were stained with cytokeratin antibody.

Drosophila and mammalian cell cultures

S2R+ cells were propagated in *Drosophila* Schneider's Medium (GIBCO) supplemented with 10% FBS and antibiotics. For co-immunoprecipitation assays, FLAG-Sd and Myc-Tgi were constructed in the pAc5.1/V5-HisB vector, with FLAG inserted N-terminal to Sd and Myc inserted N-terminal to Tgi. Mutations of Tondu domains and PPxY motifs were generated in Myc-Tgi using the QuickChange mutagenesis kit (Stratagene). Transfection and immunoprecipitation were carried out as described (Wu et al., 2003).

HEK293 cells were propagated in DMEM media supplemented with 10% FBS and 1% antibiotics. HA-tagged Vgl4 wildtype and Tondu1/2 mutant were constructed into pCDNA3.1 vector with the HA tag inserted N-terminal to a human Vgl4 cDNA (MGC IRAU Human ID# 2823240 from Invitrogen). Gal4-TEAD4 and *Ctgf*-luciferase were described (Zhao et al., 2008).

In vitro binding and competition assay

Purified His-TEAD and YAP were described previously (Liu-Chittenden et al., 2012). HA-Vgl4 was transiently expressed in HEK 293 cells and purified by immunoprecipitation. The protein G beads bound with or without HA-Vgl4 were incubated with 10 μM His-TEAD on ice for 30 min, washed 3 times with RIPA buffer, boiled in 2×SDS buffer and analyzed by western blotting. For competition assay, purified YAP (0, 5 or 10 μM) was added in the mixture, and incubated for 30 min on ice before washing and analysis.

ChIP assay

ChIP assay was carried out according to an established protocol (http://www.scbt.com/protocol_chromatin_immunoprecipitation_chip_assays.html). HA-Sd and FLAG-Tgi were transiently expressed in S2R+ cells. 1.5×10^7 cells were used for each immunoprecipitation. The PCR primers for *diap1* HRE are 5'acgaacacgaagaccaaa3' and 5'ctccaagccagtttgatt3'. The primers for 5'con are 5'atggtcgtgtccctgttt3' and 5'cttgaattatgctgcata3'.

Quantitative real-time PCR, immunohistochemistry and western analysis of liver tissues

Total liver RNA was extracted using TRIzol reagent (Invitrogen). Contaminating DNA from the RNA preparation was removed by TURBO DNA-*free*™ DNase Treatment (Ambion). RNA was reverse transcribed using iScript™ cDNA synthesis kit (Bio-Rad). Quantitative Real-time PCR was performed in triplicates using the iQ SYBR Green Supermix (Bio-Rad) on a iQ5 Multicolor Real-time PCR Detection System (Applied Biosystems). Relative fold differences in candidate gene expression in different experimental mouse livers were determined using $2^{-\Delta\Delta Ct}$ method (Livak and Schmittgen, 2001). *Gapdh* was used as a normalization control. Primer sequences used are available on request.

Mouse liver samples were collected, fixed overnight in 10% neutral buffered formalin solution (Sigma), embedded in paraffin and sectioned at 5 μm. Sections were stained with antibody against cytokeratin (pan-CK) (DAKO, 1:500). Secondary Ab used was SignalStain (R) Boost IHC Detection reagent (Cell Signaling), and the signals were developed with 2-Solution DAB kit (Invitrogen).

To prepare proteins lysates, mouse liver tissues were lysed with RIPA buffer (150mM NaCl, 50mM Tris-HCl (pH7.4), 1% NP-40, 0.5% sodium-deoxycholate and 0.1% SDS) supplemented with 1mM PMSF and protease inhibitor cocktail (Roche). The extracted proteins were loaded on SDS-PAGE gels, transferred onto PVDF membranes (Millipore). Primary antibodies used for Western Blotting were: mouse anti-YAP monoclonal antibody (Sigma, 1:2000), YAP65 rabbit monoclonal antibody (Epitomics, 1:1000), and mouse anti-actin antibody (Millipore, 1:25,000). Secondary antibodies used were Alexa Fluor 680 goat anti-rabbit IgG (Molecular Probes, 1:10,000), Goat anti-mouse IRDye 800CW (LI-COR, 1:10,000). Signals were quantified by LI-COR Infrared Imaging System.

Supplemental References

Dietzl,G., Chen,D., Schnorrer,F., Su,K.C., Barinova,Y., Fellner,M., Gasser,B., Kinsey,K., Oppel,S., Scheiblauer,S., Couto,A., Marra,V., Keleman,K., and Dickson,B.J. (2007). A genome-wide transgenic RNAi library for conditional gene inactivation in Drosophila. Nature *448*, 151-156.

Hamaratoglu,F., Willecke,M., Kango-Singh,M., Nolo,R., Hyun,E., Tao,C., Jafar-Nejad,H., and Halder,G. (2006). The tumour-suppressor genes NF2/Merlin and Expanded act through Hippo signalling to regulate cell proliferation and apoptosis. Nat. Cell Biol. *8*, 27-36.

Livak,K.J. and Schmittgen,T.D. (2001). Analysis of relative gene expression data using real-time quantitative PCR and the 2(-Delta Delta C(T)) Method. Methods *25*, 402-408.

Neto-Silva,R.M., de,B.S., and Johnston,L.A. (2010). Evidence for a growth-stabilizing regulatory feedback mechanism between Myc and Yorkie, the Drosophila homolog of Yap. Dev. Cell *19*, 507-520.

Ni,J.Q., Liu,L.P., Binari,R., Hardy,R., Shim,H.S., Cavallaro,A., Booker,M., Pfeiffer,B.D., Markstein,M., Wang,H., Villalta,C., Laverty,T.R., Perkins,L.A., and Perrimon,N. (2009). A Drosophila resource of transgenic RNAi lines for neurogenetics. Genetics *182*, 1089-1100.

Xu,T., Wang,W., Zhang,S., Stewart,R.A., and Yu,W. (1995). Identifying tumor suppressors in genetic mosaics: The Drosophila lats gene encodes a putative protein kinase. Development *121*, 1053-1063.